Structure Genome: Fill the Gap between Materials Genome and Structural Analysis

Wenbin Yu[*]

A new concept, Structure Genome (SG), is proposed to fill the gap between materials genome and structural analysis. SG acts as the basic building block of the structure connecting materials to structures and the mechanics of SG governs the necessary information to link materials genome and structural analysis. SG also enables a powerful approach to construct efficient yet high-fidelity constitutive models for composite structures over multiple length scales. No apriori assumptions will be used in the formulation and multiscale constitutive modeling is mathematically decoupled from the structural analysis. A general-purpose computer code called SwiftComp$^{\text{TM}}$ is developed to implement the mechanics of Structure Genome along with various examples to demonstrate its application and power. SwiftComp$^{\text{TM}}$ can be used as plug-in for commercial finite element codes to treat composites as "black aluminum" in structural design and analysis with negligible loss of accuracy.

I. Introduction

The recently launched Materials Genome Initiative (MGI),[1] resonating the challenges pointed out earlier in the National Research Council report on Integrated Computational Materials Engineering (ICME),[2] aims to deliver the required infrastructure and training to accelerate discovery, developing, manufacturing, and deploying of advanced materials in a more expeditious and economical way. It is true that accelerating the pace of discovery and deployment of advanced materials is crucial to achieving global competitiveness as materials with nonexisting properties will bring transformative changes in science and technology. However, material by definition is a matter from which a thing can be made of. For example, structural materials are substances used to make structures. Ultimately speaking, it is not the material performance, but the structural performance or rather system performance we are after. Thus, materials genome must integrate with structural analysis to maximize the benefits of accelerated development of advanced structural materials to be delivered by MGI and ICME.

Nowadays, structural analyses are routinely carried out using the finite element analysis (FEA) in terms of three-dimensional (3D) solid elements, two-dimensional (2D) plate or shell elements or one-dimensional (1D) beam elements (see Figure 1). For structures made of isotropic homogeneous materials, material properties characterized in materials genome are direct inputs for solid elements, and these properties combined with geometric properties of the structure can be used for plate/shell/beam elements. This implies that materials genome can be directly linked with structural analysis. However, such simplicity does not exist for structures made of composites which are usually anisotropic and heterogeneous. Consider structural analysis of the UH-60 (8 ton helicopter) all composite rotor blade. The blade is of length 8.6 m, and chord 0.72 m. Main D-spar is composed of 60 graphite/epoxy plies, and each ply has thickness of 125 μm. To directly use the properties of graphite/epoxy composite tape delivered by materials genome in structural analysis, we need to use at least one 3D solid element through the ply thickness. Supposing we use 20-noded brick elements with a 1 to 10 thickness-length ratio, it is estimated that around 11.5 billions of degrees of freedom is needed for the blade analysis.[3] Such a huge FEA model is too costly for effective structural design and analysis. The standard practice in helicopter industry is to model rotor blades as beams.[4] To this end, models are needed to take the material properties out of materials genome as inputs to compute the beam properties needed for the structural analysis and recover the 3D stress fields within the original material for failure prediction

---

[*]Associate Professor, School of Aeronautics and Astronautics, Purdue University, West Lafayette, Indiana 47907-2045. Associate Fellow, AIAA. Fellow, ASME.
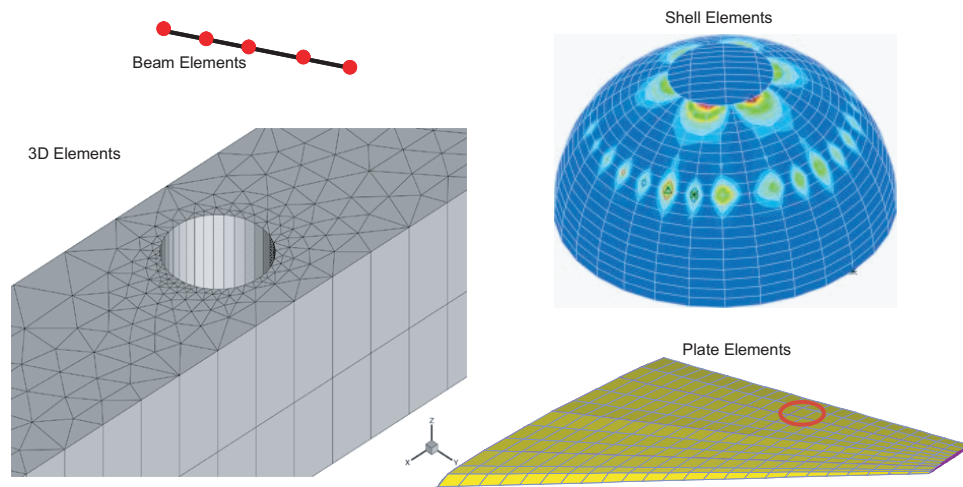
American Institute of Aeronautics and Astronautics

Figure 1. Typical structural elements

according to the allowables and failure criteria characterized by materials genome. Clearly there is a gap existing between materials genome and structural analysis.

In the past several decades, many models have been proposed to fill this gap, including both micromechanics models and structural mechanics models. These models are mainly based on various apriori assumptions. Models are either efficient but too simplistic to be predictive, or accurate but too computationally intensive to be used for effective design. These models usually cannot be used in general industrial settings particularly in the situations where the apriori assumptions will be violated. Moreover, structural mechanics models are not seamlessly unified with micromechanics models, creating difficulty for rigorous modeling of composite structures which are multiscale in nature. The present modeling capabilities for realistic composite structures are still very limited, and lagging much behind of their manufacturing techniques. For example, the recent world-wide failure analysis proved that prediction of strength for composites laminates, one of the simplest composite structures, has been elusive.[5, 6] Nevertheless, we have been successfully designed and manufactured composites in many engineering systems. We do so with the conservative Edisonian approach based on exhaustive testings. This not only attributes to the expensive development cost of composites relative to conventional materials, but also causes significant delay in time-to-market of a product.

It is thus encouraging to see that ICME and MGI try to improve our modeling capability through an integrated computational framework. However, one should be careful about what integrated computational framework entails for predictive modeling. Simply linking models at different scales and streamlining information passing between different models are not sufficient. Unpinning theory must be formulated in such a way that provides a unified way for the passing of information between models. And also material modeling must be performed with the corresponding structural analysis in mind. This is particularly true for composites as the traditional boundary between materials and structures is quickly disappearing. Some modeling should be done at the material level through ICME and MGI, but some modeling must be done at the structural level. For example, for composite laminated plates, it is reasonable to expect ICME or MGI to deliver us the properties of fiber, matrix, their interfaces, and even those of each lamina (composite tapes), but it is out of the scope of ICME or MGI to obtain plate properties for the laminate for the structural analysis using plate elements.

Another significant disadvantage of most approaches to composite structural analyses is that they lack a direct connection with the analysis of structures made of isotropic homogeneous materials. FEA has been very successful and well established for design and analysis of these structures and commercial codes such as NASTRAN, ABAQUS, ANSYS, etc. are industrial standard. However, such success has not been transplanted to composite structures. The main reason is that most models for composite structures are very different from those models used for structures made of isotropic homogeneous materials and require special purpose structural elements not available in conventional FEA. Note that many commercial codes are adding a separate composites module into their packages but those modules are different analysis codes implementing special purpose structural elements. The direct connection with conventional structural elements is missing.

American Institute of Aeronautics and Astronautics

II.   Structure Genome

To fill the gap between materials genome and composite structural analysis, avoid the disadvantages of current modeling approaches of composites, and enable a direct connection with conventional FEA, this paper will present the Structure Genome (SG) concept. According to MGI[1]

> A genome is a set of *information* encoded in the language of DNA that serves as a blueprint for an organism's growth and development. The world genome, when applied in non-biological contexts, connotes a *fundamental building block* toward a larger purpose.

Motivated by this description, we define Structure Genome (SG) as the *smallest mathematical* building block (or a cell in biological contexts) of the structure containing many such building blocks. SG not only describes the matter but also carries the information bridging materials genome and structural analysis. SG is build upon the concept of the representative structural element (RSE)[7,8] to emphasize the fact that it contains all the constitutive information needed for a structure the same fashion as the genome contains all the intrinsic information for an organism's growth and development. For periodic structures, it is easy to identify the SG as described later. However, for real structures in engineering, we rely on the expert opinion of the analysts to determine what will be the smallest, representative building block of the structure. This liberal definition is intended for maximizing the freedom in choosing the SG. It can be justified from the view point of material characterization using experiments. When experimentalists want to find properties of a material, they cut representative pieces of the material according to their own judgment and do the testing to get the properties and associated statistics. As we are not doing physical experiments, SG is thus defined as the smallest *mathematical* building block.
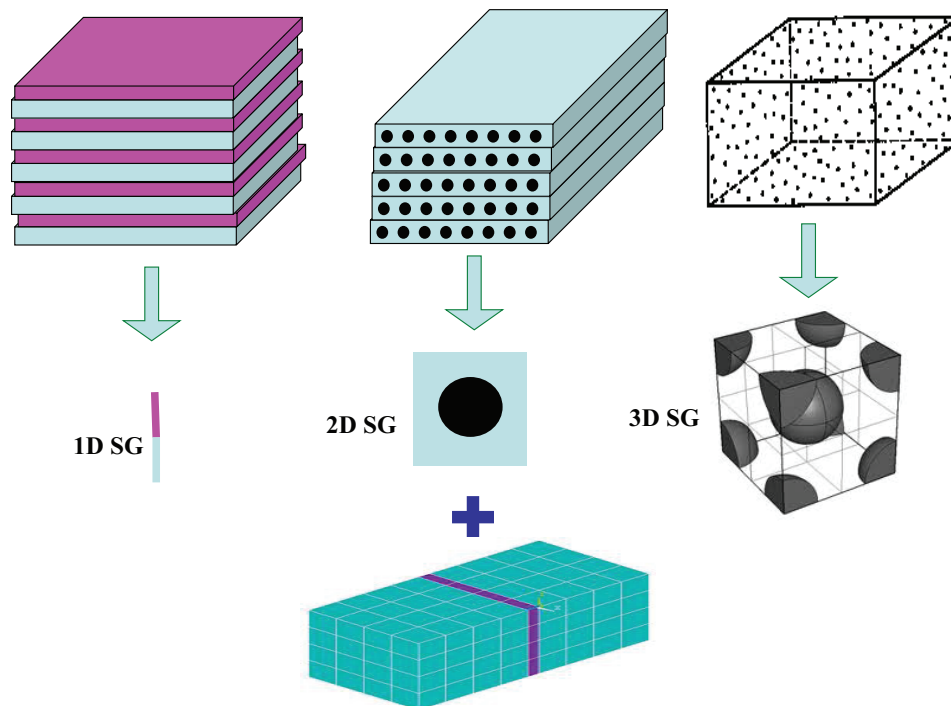

1D SG

2D SG

3D SG

Figure 2.   SG for 3D structure

A.   SG for 3D Structures

If the structural analysis uses 3D solid elements (Figure 2), SG serves a similar role as representative volume element (RVE), a concept well known in micromechanics. However, they are fundamentally different. For example, for a structure made of composites featuring 1D heterogeneity (e.g. binary composites made of two alternating layers), SG will be a straight line with two segments denoting corresponding phases. Mathematically speaking, we can repeat this straight line in plane to build the two layers of the binary

composite, then we can repeat the binary composite out of plane to build the entire structure. For a structure made of composites featuring 2D heterogeneity (e.g. continuous unidirectional fiber reinforced composites), the SG will be a 2D domain, and for a structure made of composites featuring 3D heterogeneity (e.g. particle reinforced composites), the SG will be a 3D volume. Despite of the dimensionality of SGs, the effective properties should remain 3D for the 3D macroscopic structural analysis. For example, for linear elastic behavior, one should be able to carry out a micromechanical analysis over the 1D SG to obtain the complete 6×6 stiffness matrix. Clearly, SG uses the lowest dimension, thus highest efficiency, to describe the heterogeneity, while RVE dimension is determined by heterogeneity and by what type of properties required for the macroscopic structural analysis. If 3D properties are needed for a 3D structural analysis of continuous unidirectional fiber reinforced composites, a 3D RVE is usually required [9].

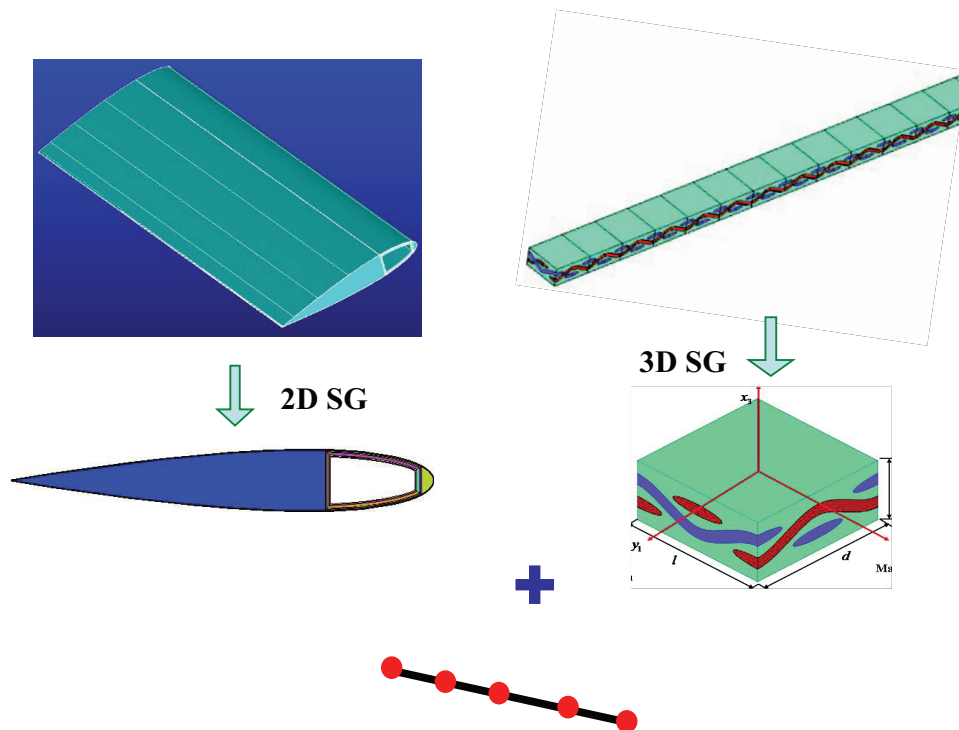## B.   SG for Dimensionally Reducible Structures

Figure 3.   SG for beam-like structures

Another feature of SG not available in RVE is that SG allows direct connection with the macroscopic structural analysis, particularly for dimensionally reducible structures which have one or two dimensions much smaller than the other dimensions. For example, the structural analysis of slender structures (beam-like structures) can use beam elements (Figure 3). If the beam has uniform cross-sections which could be made of homogeneous materials or composites, its SG is the 2D cross-sectional domain as we can repeat the cross-section along the beam reference line to build the entire structure. This inspires an *astoundingly new perspective* toward beam theories, an important traditional branch of structural mechanics. If we consider the beam reference line as a 1D continuum, every material point of this continuum has a 2D cross-section as its microstructure. In other words, *structural mechanics can be effectively viewed as a specific application of micromechanics.* If the beam is also heterogeneous in the spanwise direction, we need a 3D SG to describe the microstructure of the 1D continuum, the behavior of which is governed by the 1D macroscopic beam analysis.

If the structural analysis uses plate/shell elements, SG can also be chosen properly. For illustrative purpose, typical SGs of plate-like structures are sketched in Figure 4. If the plate-like structures feature no in-plane heterogeneities such as composite laminates, the SG is a material line along the thickness direction with each segment denoting the corresponding material of each layer. For a sandwich panel with a core cor-
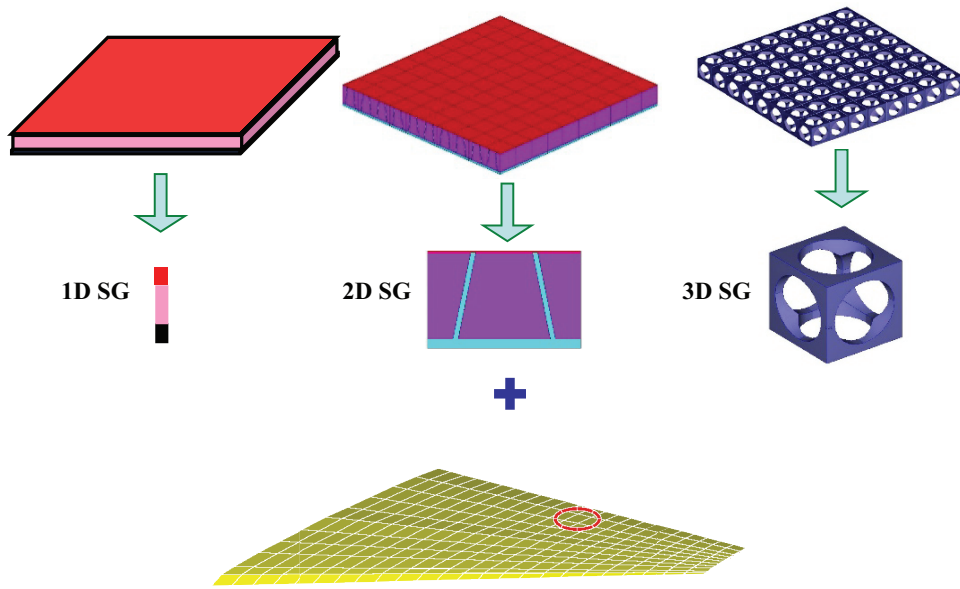
American Institute of Aeronautics and Astronautics

Figure 4. SG for plate-like structures

rugated in one direction, the SG is 2D, and if the panel is heterogeneous in both in-plane directions, the SG is 3D. Despite of different dimensions of SG, what we want out of the constitutive modeling is structural properties for the corresponding structural analysis (such as A, B, D matrices for the classical plate theory) and recovery relations to express the original 3D fields in terms of the global behavior (e.g. moments, curvatures, etc.) obtained from the plate/shell analysis. We know that theories of beams, plates, shells traditionally belong to structural mechanics, the SG concept enables us to treat them as special micromechanics theories. For a plate/shell-like structure, if we consider the reference surface as a 2D continuum, every material point of this continuum has the SG as its microstructure. Plate/shell theory constructed using the SG concept can handle buildup structures (see Figure 5) as long as their external contours look like plates or shells, that is, the thickness is much smaller than the in-plane dimensions.
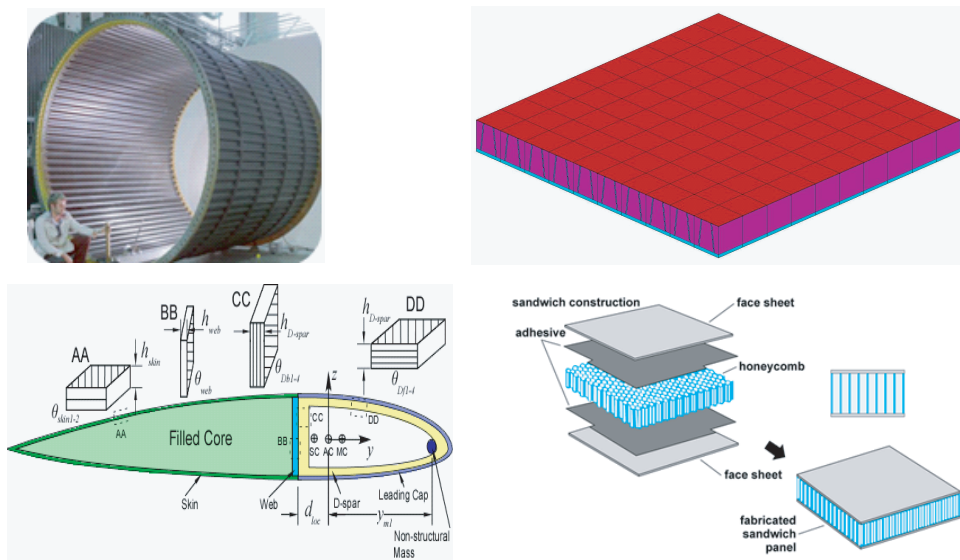

Figure 5. Typical buildup structures

Clearly SG can serve as the fundamental building block of a structure, no matter whether it is a 3D

structure, beam, plate, or shell. SG also bridges materials genome and structural analysis as SG itself is formed by materials. For SG to not merely remain as a concept, we need to develop the theory necessary to govern SG so that there is a two-way communication between materials genome and structural analysis: information from materials genome can be rigorously passed to structural analysis to predict structural performance and information from structural analysis can be passed back for material failure prediction according to materials genome. We develop such a theory with the objective to directly connect with structural analysis and minimize the loss of information from materials genome to structural analysis. As mentioned previously, structures are usually analyzed using structural elements in FEA. Underpinning each element type, there is a corresponding structural model containing three types of equations describing kinematics, kinetics, and constitutive relations. Kinematics deals with strain-displacement relations, and compatibility equations, kinetics deals with stress and equations of motion. Constitutive relations deal with stress-strain relations. Both kinematics and kinetics can be formulated exactly within the framework of continuum mechanics. Constitutive relations are ultimately approximate as we are using a hypothetical continuum to approximate the underling atomic structure of matter. Some criterion is needed for us to minimize the loss of information between materials genome and structural analysis. For elastic materials, this can be achieved by minimizing the difference between the strain energy of the materials stored in SG and that stored in the structural model of structural analysis. The mechanics of Structure Genome is derived below.

III.   Mechanics of Structure Genome

SG serves as the link of the original heterogeneous structures with microscopic details and the hypothetical homogeneous continuum used in the macroscopic structural analysis. Thus, we need to formulate its mechanics in such a way that the kinematics and energetics of the original heterogeneous structure can be expressed in terms of those of the final macroscopic structural model. Note that the final macroscopic homogenized structures are imaginary and are created by analysts to approximate the original heterogeneous structures. For this very reason, we call the final macroscopic homogenized structure as the macroscopic structural model.

A.   Kinematics

The first step in formulating the mechanics of SG is to express the kinematics, including the displacement field and the strain field, of the original heterogeneous structures in terms of those of the macroscopic structural model. Although the SG concept is applicable to heterogeneous structures made of materials admitting general continuum description such as the Cosserat continuum,[10] we are focusing on materials admitting the Cauchy continuum description: the displacement field in a 3D space is described in terms of three translations and the corresponding strain field can be defined in terms of the stretch tensor obtained through the polar decomposition of the deformation gradient tensor.

Let us use x_i, called macro coordinates here, to denote the coordinates describing the original heterogeneous structure. The coordinates could be general curvilinear coordinates. However, without loss of generality, we choose an orthogonal system of arc-length coordinates. If the structure is dimensionally reducible, some of the macro coordinates x_α, called eliminated coordinates here, correspond to the dimensions eliminated in the macroscopic structural model. (Here and throughout the paper, Greek indices assume values corresponding to the eliminated macro coordinates, Latin indices k, l, m assume values corresponding to the macro coordinates remaining in the macroscopic structural model, and other Latin indices assume 1, 2, 3. Repeated indices are summed over their range except where explicitly indicated).

For beam-like structures, only x_1, describing the beam reference line, will remain in the final beam model, and x_2, x_3, the cross-sectional coordinates, will be the eliminated coordinates; for plate/shell-like structures, x_1 and x_2, describing the plate/shell reference surface, remain in the final plate/shell model, and x_3, the thickness coordinate, will be the eliminated coordinate. For this reason, we also call the beam model as 1D continuum model as all the unknown fields are functions of x_1 only although the 1D beam model could predict 3D behavior such as translations in three directions. Similarly, we call the plate/shell model as 2D continuum model as all the unknown fields are functions of x_1 and x_2 although the 2D plate/shell model can predict 3D behavior.

In view of the fact that the size of SG is much smaller than the overall size of the macroscopic structure, we introduce a set of micro coordinates $y_i = x_i/\varepsilon$ with ε being a small parameter to describe the SG. This

American Institute of Aeronautics and Astronautics

basically enables a zoom-in view of the SG at the size similar as the macroscopic structure. If the SG is 1D, only y_3 is needed; if the SG is 2D, y_2 and y_3 are needed; if the SG is 3D, all three coordinates y_1, y_2, y_3 are needed.

In multiscale structural modeling, it is postulated that all the information can be obtained from the SG in combination with the macroscopic structural model. In other words, a field function of the original heterogeneous structure can be generally written as a function of the macro coordinates x_k which remain in the macroscopic structural model and the micro coordinates y_j. The partial derivative of a function $f(x_k, y_j)$ can be expressed as

$$\frac{\partial f(x_k, y_j)}{\partial x_i} = \frac{\partial f(x_k, y_j)}{\partial x_i}|_{y_j=\text{const}} + \frac{1}{\varepsilon}\frac{\partial f(x_k, y_j)}{\partial y_i}|_{x_k=\text{const}} \equiv f_{,i} + \frac{1}{\varepsilon}f_{|i} \tag{1}$$

Note ε is just a book keeping parameter here to facilitate the asymptotic analysis. It has no significance in the numerical implementation. Choosing an ε will fix the corresponding SG domain. εy_i together remain invariant as equal to x_i.

Letting $\boldsymbol{b}_k$ denote the tangent vector to x_k for the undeformed configuration, one is then free to chose $\boldsymbol{b}_\alpha$ tangent to x_α to form an orthonormal triad $\boldsymbol{b}_i$. Note $\boldsymbol{b}_i$ chosen this way are functions of x_k only. For example, for beam-like structures, we chose $\boldsymbol{b}_1$ to be tangent to the beam reference line x_1, and $\boldsymbol{b}_2$ and $\boldsymbol{b}_3$ as unit vectors tangent to the cross-sectional coordinates x_α. We can describe the position of any material point of the heterogeneous structure by its position vector $\boldsymbol{r}$ relative to a point O fixed in an inertial frame such that

$$\boldsymbol{r}(x_k, y_\alpha) = \boldsymbol{r}_o(x_k) + \varepsilon y_\alpha \boldsymbol{b}_\alpha(x_k) \tag{2}$$

where $\boldsymbol{r}_o$ is the position vector from O to a material point of the macroscopic structural model. Note here x_k denote only those coordinates remaining in the final macroscopic structural model, and y_α correspond to eliminated coordinates x_α. Repeated index implies summation over its own range. Because x_k is the arc-length coordinate, we have

$$\boldsymbol{b}_k = \frac{\partial \boldsymbol{r}_o}{\partial x_k} \tag{3}$$

For beam-like structures, the undeformed configuration can be described as

$$\boldsymbol{r}(x_1, y_2, y_3) = \boldsymbol{r}_o(x_1) + \varepsilon y_2 \boldsymbol{b}_2(x_1) + \varepsilon y_3 \boldsymbol{b}_3(x_1) \tag{4}$$

because the dimensions along x_2 and x_3, corresponding to εy_2 and εy_3, are eliminated in the macroscopic structural model, no matter whether the SG is 2D or 3D (see Figure 3).

For plate/shell-like structures, the undeformed configuration can be described as

$$\boldsymbol{r}(x_1, x_2, y_3) = \boldsymbol{r}_o(x_1, x_2) + \varepsilon y_3 \boldsymbol{b}_3(x_1, x_2) \tag{5}$$

because the thickness dimension along x_3, corresponding to εy_3, is eliminated in the macroscopic structural model, no matter whether the SG is 1D, 2D, or 3D (see Figure 4).

For 3D structures, the undeformed configuration can be described as

$$\boldsymbol{r}(x_1, x_2, x_3) = \boldsymbol{r}_o(x_1, x_2, x_3) \tag{6}$$

because all the macro coordinates remain in the macroscopic structural model, no matter whether the SG is 1D, 2D, or 3D (see Figure 2).

When the heterogeneous structure deforms, the particle that had position vector $\boldsymbol{r}$ in the undeformed configuration now has position vector $\boldsymbol{R}$ in the deformed configuration, such as

$$\boldsymbol{R}(x_k, y_j) = \boldsymbol{R}_o(x_k) + \varepsilon y_\alpha \boldsymbol{B}_\alpha(x_k) + \varepsilon w_i(x_k, y_j)\boldsymbol{B}_i(x_k) \tag{7}$$

where $\boldsymbol{R}_o$ denotes the position vector of the deformed homogenized structure, y_j are the micro coordinates used to describe the SG, $\boldsymbol{B}_i$ forms a new orthonormal triad for the deformed configuration, and εw_i are fluctuating functions introduced to accommodate all possible deformation other than those described by $\boldsymbol{R}_o$ and $\boldsymbol{B}_i$. The small parameter ε is added due to traditional reasons. But as it is mentioned previously, it is not a number of significance and εw_i remain as the unique solution. Note w_i are usually called warping functions in structural mechanics and we call them as fluctuating functions for the reason that structural

American Institute of Aeronautics and Astronautics

mechanics can be viewed as a special application of micromechanics using the concept of SG. $\boldsymbol{B}_i$ can be related with $\boldsymbol{b}_i$ through a direction cosine matrix, $C_{ij} = \boldsymbol{B}_i \cdot \boldsymbol{b}_j$, subject to the requirement that these two triads are the same in the undeformed configuration.

For beam-like structures featuring 2D SGs, the deformed configuration can be described as

$$\boldsymbol{R}(x_1, y_2, y_3) = \boldsymbol{R}_o(x_1) + \varepsilon y_2 \boldsymbol{B}_2(x_1) + \varepsilon y_3 \boldsymbol{B}_3(x_1) + \varepsilon w_i(x_1, y_2, y_3) \boldsymbol{B}_i(x_1) \tag{8}$$

For beam-like structures featuring 3D SGs, the deformed configuration can be described as

$$\boldsymbol{R}(x_1, y_1, y_2, y_3) = \boldsymbol{R}_o(x_1) + \varepsilon y_2 \boldsymbol{B}_2(x_1) + \varepsilon y_3 \boldsymbol{B}_3(x_1) + \varepsilon w_i(x_1, y_1, y_2, y_3) \boldsymbol{B}_i(x_1) \tag{9}$$

For plate/shell-like structures featuring 1D SGs, the deformed configuration can be described as

$$\boldsymbol{R}(x_1, x_2, y_3) = \boldsymbol{R}_o(x_1, x_2) + \varepsilon y_3 \boldsymbol{B}_3(x_1, x_2) + \varepsilon w_i(x_1, x_2, y_3) \boldsymbol{B}_i(x_1, x_2) \tag{10}$$

For plate/shell-like structures featuring 2D SGs, the deformed configuration can be described as

$$\boldsymbol{R}(x_1, x_2, y_2, y_3) = \boldsymbol{R}_o(x_1, x_2) + \varepsilon y_3 \boldsymbol{B}_3(x_1, x_2) + \varepsilon w_i(x_1, x_2, y_2, y_3) \boldsymbol{B}_i(x_1, x_2) \tag{11}$$

For plate/shell-like structures featuring 3D SGs, the deformed configuration can be described as

$$\boldsymbol{R}(x_1, x_2, y_1, y_2, y_3) = \boldsymbol{R}_o(x_1, x_2) + \varepsilon y_3 \boldsymbol{B}_3(x_1, x_2) + \varepsilon w_i(x_1, x_2, y_1, y_2, y_3) \boldsymbol{B}_i(x_1, x_2) \tag{12}$$

For 3D structures featuring 1D SGs, the deformed configuration can be described as

$$\boldsymbol{R}(x_1, x_2, x_3, y_3) = \boldsymbol{R}_o(x_1, x_2, x_3) + \varepsilon w_i(x_1, x_2, x_3, y_3) \boldsymbol{B}_i(x_1, x_2, x_3) \tag{13}$$

For 3D structures featuring 2D SGs, the deformed configuration can be described as

$$\boldsymbol{R}(x_1, x_2, x_3, y_2, y_3) = \boldsymbol{R}_o(x_1, x_2, x_3) + \varepsilon w_i(x_1, x_2, x_3, y_2, y_3) \boldsymbol{B}_i(x_1, x_2, x_3) \tag{14}$$

For 3D structures featuring 3D SGs, the deformed configuration can be described as

$$\boldsymbol{R}(x_1, x_2, x_3, y_1, y_2, y_3) = \boldsymbol{R}_o(x_1, x_2, x_3) + \varepsilon w_i(x_1, x_2, x_3, y_1, y_2, y_3) \boldsymbol{B}_i(x_1, x_2, x_3) \tag{15}$$

Note in Eq. (7), we actually express $\boldsymbol{R}$ in terms of $\boldsymbol{R}_o$, $\boldsymbol{B}_i$, and w_i, which is six times redundant. Six constraints are needed to ensure a unique mapping. These constraints are directly related with how we define $\boldsymbol{R}_o$ and $\boldsymbol{B}_i$ in terms of $\boldsymbol{R}$. For example, it is natural for us to define

$$\boldsymbol{R}_o = \langle\langle \boldsymbol{R} \rangle\rangle - \langle\langle \varepsilon y_\alpha \rangle\rangle \, \boldsymbol{B}_\alpha(x_k) \tag{16}$$

where $\langle\langle \cdot \rangle\rangle$ indicates average over SG. If y_α is chosen such that $\langle\langle \varepsilon y_\alpha \rangle\rangle = 0$, position vector of a material point in the macroscopic structural model $\boldsymbol{R}_o$ is defined as the average of the position vector of the original heterogeneous structure. This definition implies following three constraints on the fluctuating functions:

$$\langle\langle w_i \rangle\rangle = 0 \tag{17}$$

The other three constraints can be used to specify $\boldsymbol{B}_i$ in a certain fashion. For 3D structures, we already have three constraints from the definition $\boldsymbol{B}_k = \boldsymbol{R}_{o,k}$.

For plate/shell-like structures, we can select $\boldsymbol{B}_3$ in such a way that

$$\boldsymbol{B}_3 \cdot \boldsymbol{R}_{o,1} = 0 \qquad \boldsymbol{B}_3 \cdot \boldsymbol{R}_{o,2} = 0 \tag{18}$$

which provides two constraints implying that we choose $\boldsymbol{B}_3$ normal to the reference surface of the deformed plate/shell. It should be noted that this choice has nothing to do with the well-known Kirchhoff hypothesis. In the Kirchhoff assumption, the transverse normal can only rotate rigidly without any local deformation. However, in the present formulation, we allow all possible deformation, classifying all deformation other than those described by $\boldsymbol{R}_o$ and $\boldsymbol{B}_i$ in terms of the fluctuating function $w_i \boldsymbol{B}_i$. The last constraint can be specified by the rotation of $\boldsymbol{B}_\alpha$ around $\boldsymbol{B}_3$ such that

$$\boldsymbol{B}_1 \cdot \boldsymbol{R}_{o,2} = \boldsymbol{B}_2 \cdot \boldsymbol{R}_{o,1} \tag{19}$$

This constraint actually defines the macro strains for a plate/shell model as defined in Eq. (48) later to be symmetric.

For beam-like structures, we can select $\boldsymbol{B}_\alpha$ in such a way that

$$\boldsymbol{B}_2 \cdot \boldsymbol{R}_{o,1} = 0 \qquad \boldsymbol{B}_3 \cdot \boldsymbol{R}_{o,1} = 0 \tag{20}$$

which provides two constraints implying that we choose $\boldsymbol{B}_1$ to be tangent to the reference line of deformed beam. Note that this choice is not the well-known Euler-Bernoulli assumption as the present formulation allows us to describe all the deformation of the cross-section. We can also prescribe the rotation of $\boldsymbol{B}_\alpha$ around $\boldsymbol{B}_1$ such that

$$\boldsymbol{B}_3 \cdot \frac{\partial \boldsymbol{R}}{\partial x_2} - \boldsymbol{B}_2 \cdot \frac{\partial \boldsymbol{R}}{\partial x_3} = 0 \tag{21}$$

which implies the following constraint on the fluctuating functions

$$\left\langle \langle w_{2|3} - w_{3|2} \rangle \right\rangle = 0 \tag{22}$$

This constraint actually defines the twist angle of the macroscopic beam model in terms of the original position vector as pointed out in Ref. [4].

Thus the fluctuating functions are constrained according to Eq. (17) for 3D structures or plate/shell-structures, for beam structures, they are also constrained according to Eq. (22).

If the original heterogeneous structure is made of materials described using a Cauchy continuum and if the local rotation (the real rotation of a material point of the original heterogeneous structure subtracting the rotation needed for bringing $\mathbf{b}_i$ to $\mathbf{B}_i$) is small, it is convenient to use the Jauman-Biot-Cauchy strain according to the decomposition of rotation tensor.[11]

$$\Gamma_{ij} = \frac{1}{2} \left(F_{ij} + F_{ji} \right) - \delta_{ij} \tag{23}$$

where δ_{ij} is the Kronecker symbol and F_{ij} is the mixed-basis component of the deformation gradient tensor defined as

$$F_{ij} = \mathbf{B}_i \cdot \mathbf{G}_a \mathbf{g}^a \cdot \mathbf{b}_j = \mathbf{B}_i \cdot \left(\mathbf{G}_k \mathbf{g}^k + \mathbf{G}_\alpha \mathbf{g}^\alpha \right) \cdot \mathbf{b}_j \tag{24}$$

Here $\mathbf{g}^a$ are the 3D contravariant base vectors of the undeformed configuration and $\mathbf{G}_a$ are the 3D covariant basis vectors of the deformed configuration.

The contravariant base vector $\mathbf{g}^a$ is defined as

$$\mathbf{g}^a = \frac{1}{2\sqrt{g}} e_{aij} \boldsymbol{g}_i \times \boldsymbol{g}_j \tag{25}$$

with e_{aij} as the 3D permutation symbol and

$$\boldsymbol{g}_i = \frac{\partial \boldsymbol{r}}{\partial x_i} \tag{26}$$

as the covariant base vector of the undeformed configuration. g is the determinant of the metric tensor of the undeformed configuration, defined as

$$g = \det(\boldsymbol{g}_i \cdot \boldsymbol{g}_j) \tag{27}$$

From the undeformed configuration in Eq. (2), corresponding to the remaining macro coordinate x_k, we obtain the covariant base vector as

$$\boldsymbol{g}_k = \frac{\partial \boldsymbol{r}}{\partial x_k} = \boldsymbol{b}_k + \varepsilon y_\alpha \frac{\partial \boldsymbol{b}_\alpha}{\partial x_k} = \boldsymbol{b}_k + \varepsilon y_\alpha \boldsymbol{k}_k \times \boldsymbol{b}_\alpha = \boldsymbol{b}_k + e_{i\alpha j} \varepsilon y_\alpha k_{ki} \boldsymbol{b}_j \tag{28}$$

Here $\boldsymbol{k}_k = k_{ki} \boldsymbol{b}_i$ is the initial curvature vector corresponding to the remaining macro coordinate x_k. This definition is consistent with those defined for initial curvatures of shells in Ref. [12], $k_{kl}^{2\mathrm{D}}$, if we let

$$k_{kl}^{2\mathrm{D}} = \alpha_{lm} k_{km} \qquad k_{k3}^{2\mathrm{D}} = k_{k3} \tag{29}$$

with α_{lm} as the 2D permutation symbol so that $\alpha_{11} = \alpha_{22} = 0, \alpha_{12} = -\alpha_{21} = 1$.

American Institute of Aeronautics and Astronautics

From the undeformed configuration in Eq. (2), corresponding to the eliminated macro coordinate x_α, we obtain the covariant base vector as

$$\boldsymbol{g}_\alpha = \frac{\partial \boldsymbol{r}}{\partial x_\alpha} = \frac{\partial \varepsilon y_\alpha}{\partial x_\alpha} \boldsymbol{b}_\alpha = \boldsymbol{b}_\alpha \tag{30}$$

Specifically, for beam-like structures, we have

$$\mathbf{g}_1 = (1 - \varepsilon y_2 k_{13} + \varepsilon y_3 k_{12})\mathbf{b}_1 - \varepsilon y_3 k_{11}\mathbf{b}_2 + \varepsilon y_2 k_{11}\mathbf{b}_3 \tag{31}$$

$$\mathbf{g}_2 = \mathbf{b}_2 \tag{32}$$

$$\mathbf{g}_3 = \mathbf{b}_3 \tag{33}$$

$$\sqrt{g} = 1 - \varepsilon y_2 k_{13} + \varepsilon y_3 k_{12} \tag{34}$$

$$\mathbf{g}^1 = \frac{1}{\sqrt{g}}\mathbf{b}_1 \tag{35}$$

$$\mathbf{g}^2 = \mathbf{b}_2 + \frac{\varepsilon y_3 k_{11}}{\sqrt{g}}\mathbf{b}_1 \tag{36}$$

$$\mathbf{g}^3 = \mathbf{b}_3 - \frac{\varepsilon y_2 k_{11}}{\sqrt{g}}\mathbf{b}_1 \tag{37}$$

For prismatic beams, $k_{11} = k_{12} = k_{13} = 0$, and $\boldsymbol{g}_i = \boldsymbol{g}^i = \boldsymbol{b}_i$.

For plate/shell-like structures, one is free to chose the lines of curvatures to be the arc-length coordinates x_1 and x_2, so that $k_{11} = k_{22} = 0$. If such a choice is made, the covariant base vectors can be obtained in the following simple form:

$$\mathbf{g}_1 = (1 + \varepsilon y_3 k_{12})\mathbf{b}_1 \tag{38}$$

$$\mathbf{g}_2 = (1 - \varepsilon y_3 k_{21})\mathbf{b}_2 \tag{39}$$

$$\mathbf{g}_3 = \mathbf{b}_3 \tag{40}$$

$$\sqrt{g} = (1 + \varepsilon y_3 k_{12})(1 - \varepsilon y_3 k_{21}) \tag{41}$$

$$\mathbf{g}^1 = \frac{\mathbf{b}_1}{1 + \varepsilon y_3 k_{12}} \tag{42}$$

$$\mathbf{g}^2 = \frac{\mathbf{b}_2}{1 - \varepsilon y_3 k_{21}} \tag{43}$$

$$\mathbf{g}^3 = \mathbf{b}_3 \tag{44}$$

For plates, $k_{12} = k_{21} = 0$, we have $\boldsymbol{g}_i = \boldsymbol{g}^i = \boldsymbol{b}_i$.

For 3D structures, we have $\boldsymbol{g}_i = \boldsymbol{g}^i = \boldsymbol{b}_i$ according to Eq. (6).

The 3D covariant basis vectors of the deformed configuration $\mathbf{G}_i$ are defined as

$$\boldsymbol{G}_i = \frac{\partial \boldsymbol{R}}{\partial x_i} \tag{45}$$

From the deformed configuration in Eq. (7), corresponding to the remaining macro coordinate x_k, we obtain the covariant base vector $\mathbf{G}_k$ as

$$\boldsymbol{G}_k = \frac{\partial \boldsymbol{R}}{\partial x_k} = \frac{\partial \boldsymbol{R}_o}{\partial x_k} + \varepsilon y_\alpha \frac{\partial \boldsymbol{B}_\alpha}{\partial x_k} + \varepsilon \frac{\partial w_i}{\partial x_k}\boldsymbol{B}_i + \varepsilon w_i \frac{\partial \boldsymbol{B}_i}{\partial x_k} \tag{46}$$

From the deformed configuration in Eq. (7), corresponding to the eliminated macro coordinate x_α, we obtain the covariant base vector as

$$\boldsymbol{G}_\alpha = \frac{\partial \boldsymbol{R}}{\partial x_\alpha} = \frac{\partial (\varepsilon y_\beta)}{\partial x_\alpha}\boldsymbol{B}_\beta + \varepsilon \frac{\partial w_i}{\partial x_\alpha}\boldsymbol{B}_i = \boldsymbol{B}_\alpha + \frac{\partial w_i}{\partial y_\alpha}\boldsymbol{B}_i \tag{47}$$

A proper definition of the generalized strain measures for the macroscopic structural model is needed for purpose of formulating our macroscopic structural analysis in an intrinsic form. Following Refs. [4, 12, 13], we introduce the following definitions:

$$\epsilon_{kl} = \boldsymbol{B}_l \cdot \frac{\partial \boldsymbol{R}_o}{\partial x_k} - \delta_{kl}$$

$$\kappa_{ki} = \frac{1}{2}e_{iaj}\boldsymbol{B}_j \cdot \frac{\partial \boldsymbol{B}_a}{\partial x_k} - k_{ki} \tag{48}$$

where ϵ_{kl} is the Lagrangian stretch tensor and κ_{ki} is the Lagrangian curvature strain tensor. This definition corresponds to the kinematics of a nonlinear Cosserat continuum[10] which allows six independent degrees of freedom (three translations and three rotations) for each material point no matter whether the macroscopic structural model is 1D, 2D, or 3D.

For beam-like structures, these definitions reproduce the 1D generalized strain measures of the Timoshenko beam model defined in Ref. [14]. If we restrict $\boldsymbol{B}_1$ to be tangent to $\boldsymbol{R}_o$, Eq. (20), these definitions reproduce the 1D generalized strain measures of the Euler-Bernoulli beam model defined in Ref. [14].

For plate/shell-like structures, if we uses Eq. (19), we will have the symmetry $\epsilon_{12} = \epsilon_{21}$ as a constraint for the kinematics of the final plate/shell model. These definitions reproduce the 2D generalized strain measures of the Reissner-Mindlin model defined in Ref. [12]. If we further restrain $\boldsymbol{B}_3$ to be normal to the reference surface, Eq. (18), these definitions reproduce the 2D generalized strain measures of the Kirchhoff-Love model defined in Ref. [15].

For 3D structures, these definitions correspond to the natural strain measures defined in Ref. [13] for non-linear Cosserat continuum. Although the SG kinematics formulated this way has the potential to construct a Cosserat continuum model for the 3D macroscopic structural model, we will restrict ourselves to the classical Cauchy continuum model for 3D structures in this paper. In other words, we are seeking a symmetric Lagrangian stretch tensor ϵ_{kl} and negligible curvature strain tensor κ_{ki}. This can be achieved by constraining the global rotation needed for bringing $\mathbf{b}_i$ to $\mathbf{B}_i$ in a specific way, which can be illustrated more clearly using an invariant form of the definitions in Eq. (48). According to Ref. [13,16], these definitions can be rewritten as

$$\boldsymbol{\epsilon} = \boldsymbol{C}^T \cdot \boldsymbol{F} - \boldsymbol{I}$$
$$\boldsymbol{\kappa}^T = -\frac{1}{2}\boldsymbol{e} : \left(\boldsymbol{C}^T \cdot \frac{\partial \boldsymbol{C}}{\partial x_k} \boldsymbol{b}_k \right) \tag{49}$$

where $\boldsymbol{\epsilon}$ is the Lagrangian stretch tensor, $\boldsymbol{\kappa}$ the Lagrangian curvature strain tensor (or so-called wryness tensor), $\boldsymbol{C} = \boldsymbol{B}_i\boldsymbol{b}_i$ is the global rotation tensor bringing $\boldsymbol{b}_i$ to $\boldsymbol{B}_i$, $\boldsymbol{F}$ is the deformation gradient tensor, $\boldsymbol{I} = \boldsymbol{b}_i\boldsymbol{b}_i$ is the second-order identity tensor, and $\boldsymbol{e} = -\boldsymbol{I} \times \boldsymbol{I}$ is the third-order skew Ricci tensor. If we constrain the global rotation tensor $\boldsymbol{C}$ to be that can be decomposed from $\boldsymbol{F}$ according to the polar decomposition theorem such that

$$\boldsymbol{F} = \boldsymbol{C} \cdot \boldsymbol{U} \tag{50}$$

where $\boldsymbol{U}$ is a second-order positive symmetric tensor, then the definitions in Eq. (49) become

$$\boldsymbol{\epsilon} = \boldsymbol{C}^T \cdot (\boldsymbol{C} \cdot \boldsymbol{U}) - \boldsymbol{I} = \boldsymbol{U} - \boldsymbol{I}$$
$$\boldsymbol{\kappa}^T = -\frac{1}{2}\boldsymbol{e} : \left(\boldsymbol{C}^T \cdot \frac{\partial \boldsymbol{C}}{\partial x_k} \boldsymbol{b}_k \right) \tag{51}$$

Clearly, the Lagrangian stretch tensor $\boldsymbol{\epsilon}$ becomes symmetric and is the definition of Jauman-Biot-Cauchy strain tensor. Lagrangian curvature strain tensor $\boldsymbol{\kappa}$ corresponds to higher order terms, gradient of the deformation gradient, which is commonly neglected in a Cauchy continuum.

To facilitate the derivation of the covariant vectors $\boldsymbol{G}_i$, we can rewrite the definitions in Eq. (48) as

$$\frac{\partial \boldsymbol{R}_o}{\partial x_k} = \boldsymbol{B}_k + \epsilon_{kl}\boldsymbol{B}_l$$
$$\frac{\partial \boldsymbol{B}_i}{\partial x_k} = (\kappa_{kj} + k_{kj})\boldsymbol{B}_j \times \boldsymbol{B}_i \tag{52}$$

Note $\epsilon_{13} = \epsilon_{23} = 0$ for plate/shell-like structures due to Eq. (18) and $\epsilon_{12} = \epsilon_{13} = 0$ for beam-like structures due to Eq. (20).

Substituting Eq. (52) into Eq. (46), we can obtain more detailed expressions for the covariant base vectors of the deformed configuration $\boldsymbol{G}_k$ as follows:

$$\boldsymbol{G}_k = \boldsymbol{B}_k + \epsilon_{kl}\boldsymbol{B}_l + \varepsilon y_\alpha \frac{\partial \boldsymbol{B}_\alpha}{\partial x_k} + \varepsilon \frac{\partial w_l}{\partial x_k}\boldsymbol{B}_l + \varepsilon \frac{\partial w_\alpha}{\partial x_k}\boldsymbol{B}_\alpha + \varepsilon w_l \frac{\partial \boldsymbol{B}_l}{\partial x_k} + \varepsilon w_\alpha \frac{\partial \boldsymbol{B}_\alpha}{\partial x_k}$$

$$= \left(\delta_{kl} + \epsilon_{kl} + \varepsilon \frac{\partial w_l}{\partial x_k} \right)\boldsymbol{B}_l + \varepsilon\left(y_\alpha + w_\alpha \right)\frac{\partial \boldsymbol{B}_\alpha}{\partial x_k} + \varepsilon \frac{\partial w_\alpha}{\partial x_k}\boldsymbol{B}_\alpha + \varepsilon w_l \frac{\partial \boldsymbol{B}_l}{\partial x_k} \tag{53}$$

$$= \left(\delta_{kl} + \epsilon_{kl} + \varepsilon \frac{\partial w_l}{\partial x_k} \right)\boldsymbol{B}_l + \varepsilon \left[e_{ij\alpha}\left(y_\alpha + w_\alpha \right)(\kappa_{kj} + k_{kj}) + \frac{\partial w_\alpha}{\partial x_k}\delta_{\alpha i} + e_{ijl}w_l(\kappa_{kj} + k_{kj}) \right]\boldsymbol{B}_i$$

American Institute of Aeronautics and Astronautics

Note in this expressions for $\boldsymbol{G}_k$, according to Eq. (1), we have

$$\varepsilon\frac{\partial w_i(x_k,y_j)}{\partial x_k} = \varepsilon\frac{\partial w_i(x_k,y_j)}{\partial x_k}\big|_{y_j=\text{const}} + \frac{\partial w_i(x_k,y_j)}{\partial y_k}\big|_{x_k=\text{const}} \equiv \varepsilon w_{i,k} + w_{i|k} \tag{54}$$

Now, we are ready to write out the explicit expressions of $\boldsymbol{G}_i$ for beam-like structures, plate/shell-like structures, or 3D structures.

For beam-like structures, we have

$$\boldsymbol{G}_1 = \left[1 + \epsilon_{11} + \varepsilon\frac{\partial w_1}{\partial x_1} - \varepsilon(y_2 + w_2)(\kappa_{13} + k_{13}) + \varepsilon(y_3 + w_3)(\kappa_{12} + k_{12})\right]\boldsymbol{B}_1$$
$$+ \varepsilon\left[\frac{\partial w_2}{\partial x_1} - (y_3 + w_3)(\kappa_{11} + k_{11}) + w_1(\kappa_{13} + k_{13})\right]\boldsymbol{B}_2 \tag{55}$$
$$+ \varepsilon\left[\frac{\partial w_3}{\partial x_1} + (y_2 + w_2)(\kappa_{11} + k_{11}) - w_1(\kappa_{12} + k_{12})\right]\boldsymbol{B}_3$$

$$\boldsymbol{G}_2 = \frac{\partial w_1}{\partial y_2}\boldsymbol{B}_1 + \left(1 + \frac{\partial w_2}{\partial y_2}\right)\boldsymbol{B}_2 + \frac{\partial w_3}{\partial y_2}\boldsymbol{B}_3 \tag{56}$$

$$\boldsymbol{G}_3 = \frac{\partial w_1}{\partial y_3}\boldsymbol{B}_1 + \frac{\partial w_2}{\partial y_3}\boldsymbol{B}_2 + \left(1 + \frac{\partial w_3}{\partial y_3}\right)\boldsymbol{B}_3 \tag{57}$$

For plate/shell-like structures, we have

$$\boldsymbol{G}_1 = \left[1 + \epsilon_{11} + \varepsilon\frac{\partial w_1}{\partial x_1} + \varepsilon(y_3 + w_3)(\kappa_{12} + k_{12}) - \varepsilon w_2(\kappa_{13} + k_{13})\right]\boldsymbol{B}_1$$
$$+ \left[\epsilon_{12} + \varepsilon\frac{\partial w_2}{\partial x_1} - \varepsilon(y_3 + w_3)\kappa_{11} + \varepsilon w_1(\kappa_{13} + k_{13})\right]\boldsymbol{B}_2 \tag{58}$$
$$+ \varepsilon\left[\frac{\partial w_3}{\partial x_1} - w_1(\kappa_{12} + k_{12}) + w_2\kappa_{11}\right]\boldsymbol{B}_3$$

$$\boldsymbol{G}_2 = \left[\epsilon_{21} + \varepsilon\frac{\partial w_1}{\partial x_2} + \varepsilon(y_3 + w_3)\kappa_{22} - \varepsilon w_2(\kappa_{23} + k_{23})\right]\boldsymbol{B}_1$$
$$+ \left[1 + \epsilon_{22} + \varepsilon\frac{\partial w_2}{\partial x_2} - \varepsilon(y_3 + w_3)(\kappa_{21} + k_{21}) + \varepsilon w_1(\kappa_{23} + k_{23})\right]\boldsymbol{B}_2 \tag{59}$$
$$+ \varepsilon\left[\frac{\partial w_3}{\partial x_2} - w_1\kappa_{22} + w_2(\kappa_{21} + k_{21})\right]\boldsymbol{B}_3$$

$$\boldsymbol{G}_3 = \frac{\partial w_1}{\partial y_3}\boldsymbol{B}_1 + \frac{\partial w_2}{\partial y_3}\boldsymbol{B}_2 + \left(1 + \frac{\partial w_3}{\partial y_3}\right)\boldsymbol{B}_3 \tag{60}$$

For 3D structures, we have

$$\boldsymbol{G}_k = \left(\delta_{ki} + \epsilon_{ki} + \varepsilon\frac{\partial w_i}{\partial x_k}\right)\boldsymbol{B}_i \tag{61}$$

Note for 3D structures, we are focusing on a Cauchy continuum, thus the initial curvatures vanish and curvature strain tensors are higher order terms and thus neglected.

Using the expressions for $\boldsymbol{g}^a$ and $\boldsymbol{G}_a$, and dropping nonlinear terms due to the product of the curvature strains and the fluctuating functions, the 3D strain field defined in Eq. (23) can be written in the following matrix form

$$\Gamma = \Gamma_h w + \Gamma_\epsilon\bar{\epsilon} + \varepsilon\Gamma_l w + \varepsilon\Gamma_R w \tag{62}$$

where $\Gamma = \lfloor\Gamma_{11}\ \Gamma_{22}\ \Gamma_{33}\ 2\Gamma_{23}\ 2\Gamma_{13}\ 2\Gamma_{12}\rfloor^T$, $w = \lfloor w_1\ w_2\ w_3\rfloor^T$, $\bar{\epsilon}$ is a column matrix containing the generalized strain measures for the macroscopic structural model. For example, if the macroscopic structural model is a beam model we have $\bar{\epsilon} = \lfloor\epsilon_{11}\ \kappa_{11}\ \kappa_{12}\ \kappa_{13}\rfloor^T$ with ϵ_{11} denoting the extensional strain and κ_{11} the twist, κ_{12} and κ_{13} the bending curvatures. If the macroscopic structural model is a plate/shell model we have $\bar{\epsilon} = \lfloor\epsilon_{11}\ 2\epsilon_{12}\ \epsilon_{22}\ \kappa_{11}\ \kappa_{12} + \kappa_{21}\ \kappa_{22}\rfloor^T$ with $\epsilon_{\alpha\beta}$ denoting the in-plane strains and $\kappa_{\alpha\beta}$ denoting the curvature strains. To be consistent with our previous work on plate/shell modeling[12] the curvature strains

American Institute of Aeronautics and Astronautics

are defined according to Eq. (29). If the macroscopic structural model is a 3D continuum model we have $\bar{\epsilon} = \lfloor \epsilon_{11} \quad \epsilon_{22} \quad \epsilon_{33} \quad 2\epsilon_{23} \quad 2\epsilon_{13} \quad 2\epsilon_{12} \rfloor^T$ with ϵ_{ij} denoting the Biot strain measures in a Cauchy continuum.

Γ_h is an operator matrix which depends on the dimensionality of the SG. If the SG is 3D, we have

$$\Gamma_h = \begin{bmatrix} \frac{1}{\sqrt{g_1}}\frac{\partial}{\partial y_1} & 0 & 0 \\ 0 & \frac{1}{\sqrt{g_2}}\frac{\partial}{\partial y_2} & 0 \\ 0 & 0 & \frac{\partial}{\partial y_3} \\ 0 & \frac{\partial}{\partial y_3} & \frac{1}{\sqrt{g_2}}\frac{\partial}{\partial y_2} \\ \frac{\partial}{\partial y_3} & 0 & \frac{1}{\sqrt{g_1}}\frac{\partial}{\partial y_1} \\ \frac{1}{\sqrt{g_2}}\frac{\partial}{\partial y_2} & \frac{1}{\sqrt{g_1}}\frac{\partial}{\partial y_1} & 0 \end{bmatrix} \tag{63}$$

where $\sqrt{g_1} = \sqrt{g_2} = 1$ for plate-like structures or 3D structures, $\sqrt{g_1} = 1 - \varepsilon y_2 k_{13} + \varepsilon y_3 k_{12}$ and $\sqrt{g_2} = 1$ for beam-like structures, $\sqrt{g_1} = 1 + \varepsilon y_3 k_{12}$ and $\sqrt{g_2} = 1 - \varepsilon y_3 k_{21}$ for shell-like structures.

If the SG is a lower-dimensional one, one just needs to vanish the corresponding term corresponding to the micro coordinates which are not used in describing the SG. For example, if the SG is 2D, we have

$$\Gamma_h = \begin{bmatrix} 0 & 0 & 0 \\ 0 & \frac{1}{\sqrt{g_2}}\frac{\partial}{\partial y_2} & 0 \\ 0 & 0 & \frac{\partial}{\partial y_3} \\ 0 & \frac{\partial}{\partial y_3} & \frac{1}{\sqrt{g_2}}\frac{\partial}{\partial y_2} \\ \frac{\partial}{\partial y_3} & 0 & 0 \\ \frac{1}{\sqrt{g_2}}\frac{\partial}{\partial y_2} & 0 & 0 \end{bmatrix} \tag{64}$$

If the SG is 1D, we have

$$\Gamma_h = \begin{bmatrix} 0 & 0 & 0 \\ 0 & 0 & 0 \\ 0 & 0 & \frac{\partial}{\partial y_3} \\ 0 & \frac{\partial}{\partial y_3} & 0 \\ \frac{\partial}{\partial y_3} & 0 & 0 \\ 0 & 0 & 0 \end{bmatrix} \tag{65}$$

Γ_ϵ is an operator matrix the form of which depends on the macroscopic structural model. If the macroscopic structural model is the 3D Cauchy continuum model, Γ_ϵ is the 6×6 identity matrix.

If the macroscopic structural model is a beam model, we have

$$\Gamma_\epsilon = \frac{1}{\sqrt{g_1}}\begin{bmatrix} 1 & 0 & \varepsilon y_3 & -\varepsilon y_2 \\ 0 & 0 & 0 & 0 \\ 0 & 0 & 0 & 0 \\ 0 & 0 & 0 & 0 \\ 0 & \varepsilon y_2 & 0 & 0 \\ 0 & -\varepsilon y_3 & 0 & 0 \end{bmatrix} \tag{66}$$

If the macroscopic structural model is a plate/shell model, we have

$$\Gamma_\epsilon = \begin{bmatrix} \frac{1}{\sqrt{g_1}} & 0 & 0 & \frac{\varepsilon y_3}{\sqrt{g_1}} & 0 & 0 \\ 0 & 0 & \frac{1}{\sqrt{g_2}} & 0 & 0 & \frac{\varepsilon y_3}{\sqrt{g_2}} \\ 0 & 0 & 0 & 0 & 0 & 0 \\ 0 & 0 & 0 & 0 & 0 & 0 \\ 0 & 0 & 0 & 0 & 0 & 0 \\ 0 & \frac{1}{2}\left(\frac{1}{\sqrt{g_1}} + \frac{1}{\sqrt{g_2}}\right) & 0 & 0 & \frac{1}{2}\left(\frac{\varepsilon y_3}{\sqrt{g_1}} + \frac{\varepsilon y_3}{\sqrt{g_2}}\right) & 0 \end{bmatrix} \tag{67}$$

American Institute of Aeronautics and Astronautics

Note the above expression is obtained with the understanding that the difference between κ_{12} and κ_{21} is of higher order and negligible if we are not seeking a higher-order approximation of the initial curvatures.

Γ_l is an operator matrix the form of which depends on the macroscopic structural model. If the macroscopic structural model is 3D, Γ_l has the same form as Γ_h in Eq. (68) with $\frac{\partial}{\partial y_k}$ replaced with $\frac{\partial}{\partial x_k}$, that is

$$\Gamma_l = \begin{bmatrix} \frac{1}{\sqrt{g_1}}\frac{\partial}{\partial x_1} & 0 & 0 \\ 0 & \frac{1}{\sqrt{g_2}}\frac{\partial}{\partial x_2} & 0 \\ 0 & 0 & \frac{\partial}{\partial x_3} \\ 0 & \frac{\partial}{\partial x_3} & \frac{1}{\sqrt{g_2}}\frac{\partial}{\partial x_2} \\ \frac{\partial}{\partial x_3} & 0 & \frac{1}{\sqrt{g_1}}\frac{\partial}{\partial x_1} \\ \frac{1}{\sqrt{g_2}}\frac{\partial}{\partial x_2} & \frac{1}{\sqrt{g_1}}\frac{\partial}{\partial x_1} & 0 \end{bmatrix} \tag{68}$$

Of course for 3D structures, we have $\sqrt{g_1} = \sqrt{g_2} = 1$.

If the macroscopic structural model is a lower-dimensional one, one just needs to vanish the corresponding term corresponding to the macro coordinates which are not used in describing the macroscopic structural model. For example, if the macroscopic structural model is a 2D plate/shell model, we have

$$\Gamma_l = \begin{bmatrix} \frac{1}{\sqrt{g_1}}\frac{\partial}{\partial x_1} & 0 & 0 \\ 0 & \frac{1}{\sqrt{g_2}}\frac{\partial}{\partial x_2} & 0 \\ 0 & 0 & 0 \\ 0 & 0 & \frac{1}{\sqrt{g_2}}\frac{\partial}{\partial x_2} \\ 0 & 0 & \frac{1}{\sqrt{g_1}}\frac{\partial}{\partial x_1} \\ \frac{1}{\sqrt{g_2}}\frac{\partial}{\partial x_2} & \frac{1}{\sqrt{g_1}}\frac{\partial}{\partial x_1} & 0 \end{bmatrix} \tag{69}$$

If the macroscopic structural model is the 1D beam model, we have

$$\Gamma_l = \begin{bmatrix} \frac{1}{\sqrt{g_1}}\frac{\partial}{\partial x_1} & 0 & 0 \\ 0 & 0 & 0 \\ 0 & 0 & 0 \\ 0 & 0 & 0 \\ 0 & 0 & \frac{1}{\sqrt{g_1}}\frac{\partial}{\partial x_1} \\ 0 & \frac{1}{\sqrt{g_1}}\frac{\partial}{\partial x_1} & 0 \end{bmatrix} \tag{70}$$

Γ_R is an operator matrix existing only for those heterogeneous structures featuring initial curvatures. For prismatic beams, plates or 3D structures, Γ_R vanishes. For those structures having initial curvatures such as initially twisted/curved beams or shells, the form of Γ_R depends on the macroscopic structural model. If the macroscopic structural model is a 1D beam model,

$$\Gamma_R = \frac{1}{\sqrt{g_1}} \begin{bmatrix} k_{11}\left(y_3\frac{\partial}{\partial y_2} - y_2\frac{\partial}{\partial y_3}\right) & -k_{13} & k_{12} \\ 0 & 0 & 0 \\ 0 & 0 & 0 \\ 0 & 0 & 0 \\ -k_{12} & k_{11} & k_{11}\left(y_3\frac{\partial}{\partial y_2} - y_2\frac{\partial}{\partial y_3}\right) \\ k_{13} & k_{11}\left(y_3\frac{\partial}{\partial y_2} - y_2\frac{\partial}{\partial y_3}\right) & -k_{11} \end{bmatrix} \tag{71}$$

If the macroscopic structural model is a 2D shell model,

$$\Gamma_R = \begin{bmatrix} 0 & \frac{-k_{13}}{\sqrt{g_1}} & \frac{k_{12}}{\sqrt{g_1}} \\ \frac{k_{23}}{\sqrt{g_2}} & 0 & \frac{-k_{21}}{\sqrt{g_2}} \\ 0 & 0 & 0 \\ 0 & \frac{k_{21}}{\sqrt{g_2}} & 0 \\ \frac{-k_{12}}{\sqrt{g_1}} & 0 & 0 \\ \frac{k_{13}}{\sqrt{g_1}} & -\frac{k_{23}}{\sqrt{g_2}} & 0 \end{bmatrix} \tag{72}$$

B. Variational Statement for SG

Although the SG concept can be used to analyze various type of behavior of heterogeneous structures, we are instead focusing on the elastostatic behavior of the original heterogeneous structure for illustrative purpose in this paper, which is governed by the following variational statement

$$\delta U = \overline{\delta W} \tag{73}$$

δ is the usual Lagrangean variation, U is the strain energy and $\overline{\delta W}$ is the virtual work of applied loads. The bars over variations are used to indicate that the virtual quantity needs not be the variation of a functional. For a linear elastic material characterized using a 6×6 stiffness matrix D, the strain energy can be written as

$$U = \frac{1}{2} \int \frac{1}{\omega} \left\langle \Gamma^T D \Gamma \right\rangle \mathrm{d}\Omega \tag{74}$$

where Ω is the volume of the domain spanned by x_k remaining in the macroscopic structural model. The notation $\langle \bullet \rangle = \int \bullet \sqrt{g} \mathrm{d}\omega$ is used to denote a weighted integration over the domain of the SG, ω, where g is the determinant of the metric tensor of the undeformed configuration spanned by x_1, x_2, x_3, as defined previously. ω also denotes the volume of the domain spanned by y_k corresponding to the coordinates x_k remaining in the macroscopic structural model. If none of y_k are needed in the SG, then $\omega = 1$. For example, if a heterogeneous beam-like structure features a 3D SG, ω is the length of the SG in the y_1 direction, corresponding to x_1 remaining in the macroscopic beam model. If the heterogeneous beam-like structure features a 2D SG (uniform cross-section), y_1 is not needed for the SG and $\omega = 1$. If a heterogeneous plate/shell-like structure features a 3D SG, ω is the area of the SG in the $y_1 - y_2$ plane, corresponding to x_1 and x_2 remaining in the macroscopic plate/shell model. If the heterogeneous plate/shell-like structure features a 2D SG, y_2 and y_3 are needed for the SG and ω is equal to the length of SG in y_2 direction. If the heterogeneous plate/shell-like structure features a 1D SG, only y_3 is needed for the SG and $\omega = 1$. If a 3D heterogeneous structure features a 3D SG, ω is the physical volume of SG spanned by y_1, y_2, and y_3. If a 3D heterogeneous structure features a 2D SG, ω is the area of SG spanned by y_2 and y_3. If a 3D heterogeneous structure features a 1D SG, ω is the length of SG in y_3 direction.

For a Cauchy continuum, there may exist applied loads from tractions and body forces. The virtual work done by these applied loads can be calculated as

$$\overline{\delta W} = \int \frac{1}{\omega} \left(\langle \mathbf{p} \cdot \delta \mathbf{R} \rangle + \int_s \mathbf{Q} \cdot \delta \mathbf{R} \sqrt{c} \mathrm{d}s \right) \mathrm{d}\Omega \tag{75}$$

where s denotes the boundary surfaces of the SG where the traction force per unit area $\mathbf{Q} = Q_i \mathbf{B}_i$ is applied and $\mathbf{p} = p_i \mathbf{B}_i$ denotes the applied body force per unit undeformed volume. $\sqrt{c}$ is equal to 1 except for some degenerated cases where s is only a boundary curve of the SG and one of coordinates x_k is required to form the physical surfaces on which the load is applied. In this case, the differential area of the physical surface is equal to $\sqrt{c} \mathrm{d}s \mathrm{d}x_k$ with $\mathrm{d}s$ as the differential arc length along the boundary curve of SG. For example for beam-like structures featuring a 2D SG, the SG boundary is the curve encircling the cross-section, and $\sqrt{c} = \sqrt{g + \left(y_2 \frac{\mathrm{d}y_2}{\mathrm{d}s} + y_3 \frac{\mathrm{d}y_3}{\mathrm{d}s} \right)^2 k_{11}^2}$. $\delta \mathbf{R}$ is the Lagrangian variation of the displacement field in Eq. (7), such that

$$\delta \mathbf{R} = \overline{\delta q_i} \mathbf{B}_i + \varepsilon y_\alpha \delta \mathbf{B}_\alpha + \varepsilon \delta w_i \mathbf{B}_i + \varepsilon w_i \delta \mathbf{B}_i \tag{76}$$

We may safely ignore products of the fluctuating function and virtual rotation in $\delta \mathbf{R}$, because the fluctuating functions are small. The last term of the above equation is then dropped so that

$$\delta \mathbf{R} = \overline{\delta q_i} \mathbf{B}_i + \varepsilon y_\alpha \delta \mathbf{B}_\alpha + \varepsilon \delta w_i \mathbf{B}_i \tag{77}$$

The virtual displacements and rotations of the macroscopic structural model are defined as

$$\overline{\delta q_i} = \delta \mathbf{R}_o \cdot \mathbf{B}_i \qquad \delta \mathbf{B}_\alpha = \overline{\delta \psi_j} \mathbf{B}_j \times \mathbf{B}_\alpha \tag{78}$$

where $\overline{\delta q_i}$ and $\overline{\delta \psi_i}$ contain the components of the virtual displacement and rotation in the $\mathbf{B}_i$ system, respectively. They are functions of x_k only. Note $\overline{\delta \psi_j}$ are restrained to be derivable from $\overline{\delta q_i}$ and are higher order terms neglected in a 3D structure described using the Cauchy continuum.

Then we can rewrite Eq. (77) as

$$\delta \mathbf{R} = \left(\overline{\delta q_i} + \varepsilon e_{j\alpha i} y_\alpha \overline{\delta \psi_j} + \varepsilon \delta w_i \right) \mathbf{B}_i \tag{79}$$

Finally, we express the virtual work due to applied loads as

$$\overline{\delta W} = \overline{\delta W}_H + \varepsilon \overline{\delta W}^* \tag{80}$$

where $\overline{\delta W}_H$ is the virtual work not related with the fluctuating functions w_i and $\overline{\delta W}^*$ is the virtual work related with the fluctuating functions. Specifically, they are

$$\overline{\delta W}_H = \int \left(f_i \overline{\delta q_i} + m_i \overline{\delta \psi_i} \right) \mathrm{d}\Omega \qquad \overline{\delta W}^* = \int \frac{1}{\omega} \left(\langle p_i \delta w_i \rangle + \oint Q_i \delta w_i \sqrt{c} \, \mathrm{d}s \right) \mathrm{d}\Omega \tag{81}$$

with the generalized forces f_i and moments m_i defined as

$$f_i = \frac{1}{\omega} \left(\langle p_i \rangle + \int Q_i \sqrt{c} \, \mathrm{d}s \right) \qquad m_i = \frac{e_{i\alpha j}}{\omega} \left(\langle \varepsilon y_\alpha p_j \rangle + \int \varepsilon y_\alpha Q_j \sqrt{c} \, \mathrm{d}s \right) \tag{82}$$

If we assume that p_i and Q_i are independent of the fluctuating functions, then we can rewrite $\overline{\delta W}^*$ as

$$\overline{\delta W}^* = \delta \int \frac{1}{\omega} \left(\langle p_i w_i \rangle + \int Q_i w_i \sqrt{c} \, \mathrm{d}s \right) \mathrm{d}\Omega \tag{83}$$

In view of the strain energy in Eq. (74) and virtual work in Eq. (80) along with Eq. (81), the variational statement in Eq. (73) can be rewritten as

$$\int \frac{1}{\omega} \delta \left[\frac{1}{2} \langle \Gamma^T D \Gamma \rangle - \varepsilon \left(\langle p_i w_i \rangle - \int Q_i w_i \sqrt{c} \, \mathrm{d}s \right) \right] - \left(f_i \overline{\delta q_i} + m_i \overline{\delta \psi_i} \right) \mathrm{d}\Omega = 0 \tag{84}$$

If we attempt to solve this variational statement directly, we will meet the same difficulty as solving the original problem of heterogeneous structures. The main complexity comes from the fluctuating functions w_i which are unknown functions of both micro and macro coordinates. The common practice in the literature is to assume the fluctuating functions, a priori, in terms of some unknown functions (displacements, rotations, and/or strains) of x_k and some known functions of y_k, to straightforwardly reduce the original continuum model into a macroscopic structural model. However, for arbitrary heterogeneous structures made with general composites, the imposition of such ad hoc assumptions may introduce significant errors. Fortunately, variational asymptotic method (VAM)[17] provides a useful technique to obtain the fluctuating functions through an asymptotical analysis of the variational statement in Eq. (84) in terms of the small parameter ε inherent in the heterogeneous structure to construct asymptotically correct macroscopic structural models. As the last two terms in Eq. (84) are not functions of w_i, we can conclude that the fluctuating function is governed by the following variational statement instead:

$$\delta \left[\frac{1}{2} \langle \Gamma^T D \Gamma \rangle - \varepsilon \left(\langle p_i w_i \rangle - \int Q_i w_i \sqrt{c} \, \mathrm{d}s \right) \right] = 0 \tag{85}$$

which can be considered as a variational statement for the SG as it is posed over the SG domain only.

American Institute of Aeronautics and Astronautics

According to VAM, we can neglect the terms in the order of ε to construct the first approximation of the variational statement in Eq. (85) as

$$\delta \frac{1}{2} \left\langle (\Gamma_h w + \Gamma_\epsilon \bar{\epsilon})^T D (\Gamma_h w + \Gamma_\epsilon \bar{\epsilon}) \right\rangle = 0 \tag{86}$$

For very simple cases, this variational statement can be solved analytically, while for general cases we need to turn to numerical techniques such as the finite element method for solution. To this end, we need to express w using shape functions defined over SG as

$$w(x_k, y_j) = S(y_j) V(x_k) \tag{87}$$

where S represents the shape functions and V a column matrix of the nodal values of the fluctuating functions.

Substituting Eq. (87) into Eq. (86), we obtain the the following discretized version of the strain energy functional:

$$U = \frac{1}{2} \left(V^T E V + 2 V^T D_{h\epsilon} \bar{\epsilon} + \bar{\epsilon}^T D_{\epsilon\epsilon} \bar{\epsilon} \right) \tag{88}$$

where

$$E = \left\langle (\Gamma_h S)^T D (\Gamma_h S) \right\rangle \quad D_{h\epsilon} = \left\langle (\Gamma_h S)^T D \Gamma_\epsilon \right\rangle \quad D_{\epsilon\epsilon} = \left\langle \Gamma_\epsilon^T D \Gamma_\epsilon \right\rangle \tag{89}$$

Minimizing U in Eq. (88) subject to the constraints, gives us the following linear system

$$EV = -D_{h\epsilon} \bar{\epsilon} \tag{90}$$

It is clear that V will linearly depend on $\bar{\epsilon}$, and the solution can be symbolically written as

$$V = V_0 \bar{\epsilon} \tag{91}$$

Substituting Eq. (91) back into Eq. (88), we can calculate the strain energy storing in the SG as the first approximation as

$$U = \frac{1}{2} \bar{\epsilon}^T \left(V_0^T D_{h\epsilon} + D_{\epsilon\epsilon} \right) \bar{\epsilon} \equiv \frac{\omega}{2} \bar{\epsilon}^T \bar{D} \bar{\epsilon} \tag{92}$$

where $\bar{D}$ is the effective stiffness to be used in the macroscopic structural model.

Substituting the solved strain energy stored in the SG into Eq. (84), we can rewrite the variational statement governing the original heterogeneous structures as

$$\int \left[\delta \left(\frac{1}{2} \bar{\epsilon}^T \bar{D} \bar{\epsilon} \right) - f_i \overline{\delta q_i} - m_i \overline{\delta \psi_i} \right] d\Omega = 0 \tag{93}$$

This variational statement governs the macroscopic structural model as it involves only fields which are unknown functions of macro coordinates x_k. The first term is the variation of the strain energy of the macroscopic structural model and the last terms are the virtual work done by generalized forces and moments. This variational statement governs the C^1 structural elements and 3D solid elements implemented in most commercial FEA software packages.

We are not only interested in obtaining the effective stiffness and macroscopic structural behavior. We are also interested in obtaining the local fields within the original heterogeneous structure. First knowing $\bar{\epsilon}$, we can compute the fluctuating function as

$$w = S V_0 \bar{\epsilon} \tag{94}$$

The local displacement field can be obtained as

$$u_i = \bar{u}_i + \varepsilon y_\alpha (C_{\alpha i} - \delta_{\alpha i}) + \varepsilon w_j C_{ji} \tag{95}$$

where u_i is the local displacement, $\bar{u}_i$ is the macroscopic displacement.

The local strain field can be obtained as

$$\Gamma = (\Gamma_h S V_0 + \Gamma_\epsilon) \bar{\epsilon}. \tag{96}$$

The local stress field can be obtained directly using the Hooke's law as

$$\sigma = D\Gamma. \tag{97}$$

American Institute of Aeronautics and Astronautics

IV. Numerical Examples

The Mechanics of Structure Genome developed in this paper is implemented into a computer code called SwiftComp$^{\text{TM}}$ using the modern Fortran language. Although still in its early development stage, SwiftComp$^{\text{TM}}$ has demonstrated a great potential for multiscale constitutive modeling of composites as it represents a unique unified approach for modeling composites structures and materials. A few examples are used here to demonstrate the application and validity of the Mechanics of Structure Genome and the companion code SwiftComp$^{\text{TM}}$. As it can be theoretically shown that one can specialize the Mechanics of Structure Genome to reproduce the theories the author and his co-workers have developed over the years for composite beams (Variational Asymptotic Beam Sectional analysis (VABS)), composite plates/shells (Variational Asymptotic Plate And Shell analysis (VAPAS)), and micromechanics (Variational Asymptotic Method for Unit Cell Homogenization (VAMUCH)). We have verified that SwiftComp$^{\text{TM}}$ can reproduce all the results of VAMUCH, and the classical models of VABS and VAPAS. Here, we just study a few examples which have been studied before in our previous publication to demonstrate the application of SwiftComp$^{\text{TM}}$.
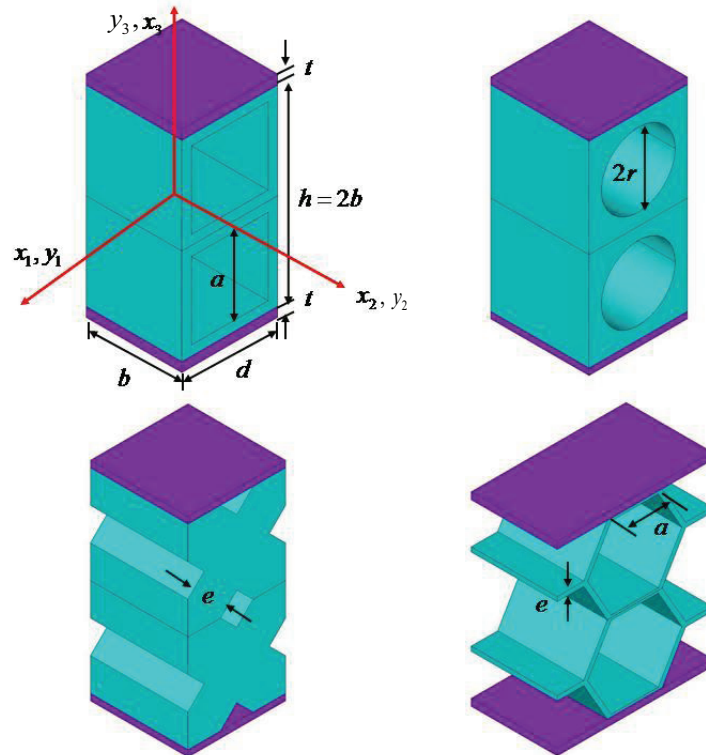

Figure 6. Structure genome for sandwich beam with various cross-sections

A. Sandwich Beam with Periodically Variable Cross-Section

The first example is to analyze a sandwich beam with periodically variable cross-section studied in Ref. [18]. The geometric parameters for each configuration are given below:

- For the sandwich beam with square holes, the geometric variables are given by $b = d = 1.5$ m, $t = 0.1$ m, $a = 1$ m (Figure 6 : top-left)

- For the sandwich beam with circular holes, the geometric variables are given by $b = d = 1.5$ m, $t = 0.1$ m, $r = 0.5614$ m (Figure 6 : top-right)

- For the sandwich beam with cross holes, the geometric variables are given by $b = d = 1.5$ m, $t = 0.1$ m, $e = 0.7071$ m (Figure 6 : bottom-left)

American Institute of Aeronautics and Astronautics

- For the sandwich beam with hexagonal holes, the geometric variables are given by $b = 1.23745$ m, $d = 2b$, $t = 0.1$ m, $a = 0.7887$ m, $e = 0.6431$ m (Figure 6 : bottom-right)

Note although all the SG in Figure 6 are uniform along y_2, the SG must be 3D as they are used to form a beam structure and y_2 is one of the cross-section domain which is finite, see Figure 7. All sandwich beams in the above cases have the same core material properties (material indicated by blue color in the figure) of $E_c = 3.5$ GPa, $\nu_c = 0.34$ and face sheet material properties (indicated by purple color in the figure) of $E_f = 70$ GPa, $\nu_c = 0.34$. Note although these beams are studied in [19], only bending stiffness is given. In fact, the effective stiffness for the classical beam model in general should be represented by a fully populated 4×4 matrix. The effective bending stiffnesses predicted by the analytical formulas in [19] and SwiftComp$^{\text{TM}}$ are listed in Table 1.

Table 1. Effective beam bending stiffness of sandwich beams predicted by different methods ($\times 10^{10}$ N.m^2)

	Ref. [19]	SwiftComp$^{\text{TM}}$
Rectangle Holes	5.669	5.576
Circular Holes	5.176	5.537
Cross Holes	5.486	5.805
Hexagon Holes	2.875	2.888

As can be observed, SwiftComp$^{\text{TM}}$ predictions are slightly different from those in [19]. However, the present approach is more versatile than that in [19] because [19] only provides analytic formulas for bending stiffness of beams made of materials characterized only by one material constant, the Young's modulus, while SwiftComp$^{\text{TM}}$ can estimate all the engineering beam constants represented by a 4×4 stiffness matrix, possibly fully populated, for the most general anisotropic materials by factorizing the coefficient material in the linear system, Eq. (90), only once.
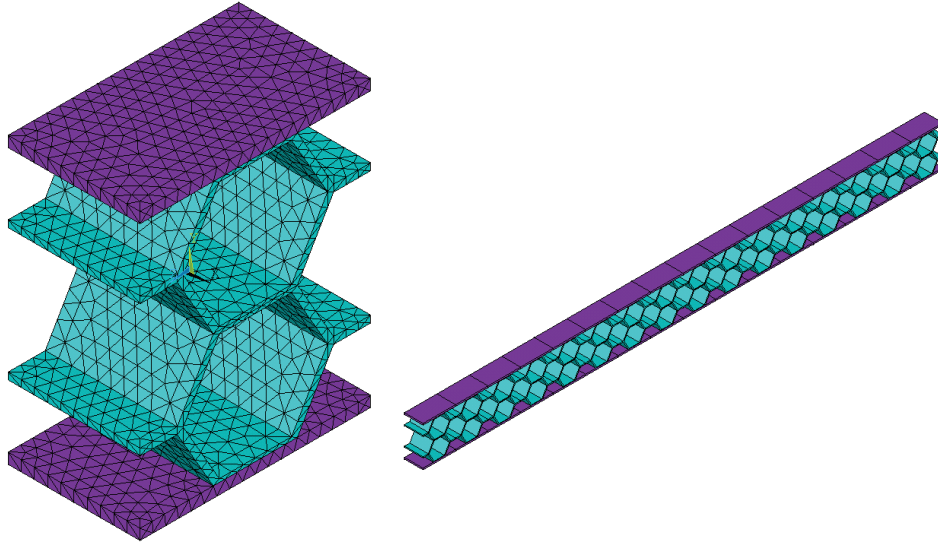

Figure 7. A sandwich beam with hexagonal holes

B.   Sandwich Panel with a Corrugated Core

The second example is to model a corrugated-core sandwich panel, a concept used for Integrated Thermal Protection System (ITPS) studied in [20, 21]. The ITPS panel along with the details of the SG is sketched in Figure 8. The geometry parameters are $t_T = 1.2$ mm, $t_B = 7.49$ mm, $t_W = 1.63$ mm, $p = 25$ mm, $d = 70$ mm, and $\theta = 85°$. Both materials are isotropic with $E_1 = 109.36$ GPa, $\nu_1 = 0.3$, $E_2 = 209.482$ GPa, $\nu_2 = 0.063$. Although 3D unit cells are needed for the study in [20], only a 2D SG is necessary for

American Institute of Aeronautics and Astronautics

SwiftComp[TM] as it is uniform along one of the in-plane directions. The effective stiffness for the classical plate model can be represented using A, B and D matrices known in classical lamination theory. Results obtained in Ref. [20] are compared with SwiftComp[TM] in Tables 2, 3 and 4. SwiftComp[TM] predictions agree very well with those in Ref. [20] with the biggest difference (around 1%) appearing for the extension-bending coupling stiffness (B_{11}). However, the present approach is much more efficient because using the approach in [20] one needs to carry out six analyses of a 3D unit cell under six different sets of boundary conditions and load conditions and postprocess the 3D stresses to compute the plate stress resultants, while using the present approach, one only needs to carry out one analysis of a 2D SG without any postprocessing.
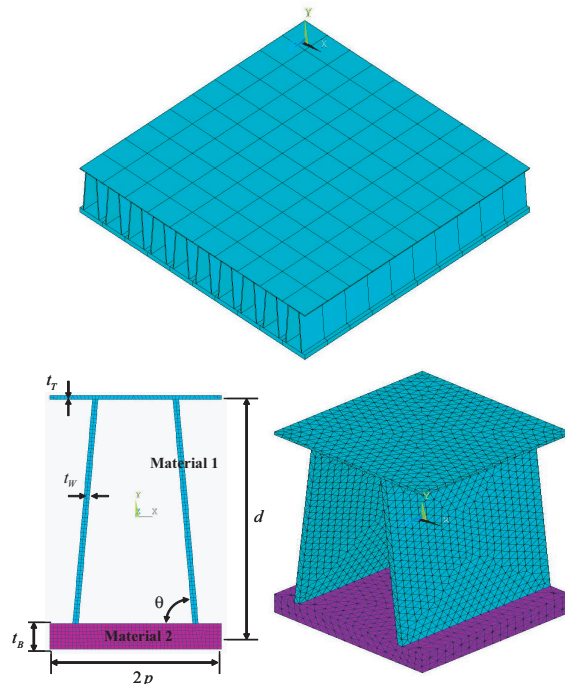

Figure 8. Sketch of the ITPS panel and its SG

Table 2. Effective extension stiffness of ITPS ($\times 10^9$ N/m)

	A_{11}	A_{13}	A_{22}	A_{33}
Ref. [20]	2.83	0.18	1.07	2.33
SwiftComp[TM]	2.80	0.18	1.08	2.33

Table 3. Effective bending stiffness of ITPS ($\times 10^6$ N.m)

	D_{11}	D_{13}	D_{22}	D_{33}
Ref. [20]	3.06	0.22	1.32	2.85
SwiftComp[TM]	3.03	0.22	1.32	2.87

V.   Conclusion

This paper introduces the concept of structure genome (SG) to bridge materials genome and structural analysis. SG facilitates a mathematical decoupling of the original complex analysis of composite structures

American Institute of Aeronautics and Astronautics

Table 4. Effective coupling stiffness of ITPS ($\times 10^6$ N)

	B_{11}	B_{13}	B_{22}	B_{33}
Ref. [20]	-71.45	-3.36	-34.05	-71.45
SwiftComp$^{\text{TM}}$	-70.67	-3.31	-34.06	-71.42

into a constitutive modeling over SG and a macroscopic structural analysis. The constitutive modeling will not only perform homogenization to obtain the constitutive relations for the macroscopic structural analysis but also perform dehomogenization to obtain the local fields within the microstructure. This paper not only formulated the mechanics of structure genome but also implemented the theory in a computer code called SwiftComp$^{\text{TM}}$. Mechanics of SG presented in this paper enables a multiscale constitutive modeling approach with the following unique features:

- Use SG to fill the gap between materials genome and structural analysis. Intellectually, SG enables us to view structural mechanics as an application of micromechanics. Technically, SG empowers us to systematically model complex buildup structures with heterogeneities of a length scale comparable to the smallest structural dimension.

- Use VAM to avoid apriori assumptions commonly invoked in other approaches, providing the most mathematical rigor and the best engineering generality.

- Decouple the original problem into two sets of analyses: a constitutive modeling and a structural analysis. This allows the structural analysis to be formulated exactly as a general (1D, 2D, or 3D) continuum, the analysis of which is readily available in commercial FEA software packages and confines all approximations to the constitutive modeling, the accuracy of which is guaranteed to be the best by VAM.

A general-purpose computer code called SwiftComp$^{\text{TM}}$ is developed to implement the Mechanics of Structure Genome along with several examples to demonstrate its application and power.

VI.   Acknowledgments

References

[1] "Materials Genome Initiative for Global Competitiveness," Tech. Rep. `http://www.whitehouse.gov/sites/default/files/microsites/ostp/materials_genome_initiative-final.pdf`, Executive Office of the President National Science and Technology Council, Washington, DC, 2011.

[2] "Integrated Computational Materials Engineering: a Transformational Discipline for Improved Competitiveness and National Security," Tech. Rep. `http://www.nap.edu/catalog.php?record_id=12199`, National Research Council, 2008.

[3] Han, S., *Integration of Flexible Multibody Dynamic Analysis with Dimensional Reduction Techniques*, Ph.D. thesis, Shanghai Jiao Tong University, 2014.

[4] Yu, W., Hodges, D. H., and Ho, J. C., "Variational Asymptotic Beam Sectional Analysis - An Updated Version," *International Journal of Engineering Science*, Vol. 59, 2012, pp. 40–64.

[5] Kaddour, A. S. and Hinton, M. J., "Evaluation of Theories for Predicting Failure in Polymer Composite Laminates under 3-D States of Stress: Part A of the Second World-Wide Failure Exercise (WWFE-II)," *Journal of Composite Materials*, Vol. 46, 2012, pp. 19 – 20.

[6] Kaddour, A. S. and Hinton, M. J., "Evaluation of Theories for Predicting Failure in Polymer Composite Laminates under 3-D States of Stress: Part B of the Second World-Wide Failure Exercise (WWFE-II)," *Journal of Composite Materials*, Vol. 47, 2013, pp. 6 – 7.

[7] Yu, W., "Unifying Structural Mechanics with Micromechanics Using the Concept of Representative Structural Element," *Proceedings of the American Society for Composites 27th Technical Conference*, Arlington, Texas, Oct. 1 – 3 2012.

[8]Yu, W., "Representative Structural Element: a New Paradigm for Multiscale Structural Modeling," *Proceedings of the 54th Structures, Structural Dynamics and Materials Conference*, AIAA, Boston, Massachusetts, Apr. 8-11 2013.

[9]Sun, C. T. and Vaidya, R. S., "Prediction of Composite Properties from a Representative Volume Element," *Composites Science and Technology*, Vol. 56, 1996, pp. 171 – 179.

[10]Cosserat, B. and Cosserat, F., *Théorie des Corps Deformables*, Hermann, Paris, 1909.

[11]Danielson, D. and Hodges, D., "Nonlinear Beam Kinematics by Decomposition of the Rotation Tensor," *Journal of Applied Mechanics*, Vol. 54, 1987, pp. 258–262.

[12]Yu, W. and Hodges, D. H., "A Geometrically Nonlinear Shear Deformation Theory for Composite Shells," *Journal of Applied Mechanics*, Vol. 71, No. 1, 2004, pp. 1 – 9.

[13]Pietraszkiewicz, W. and Eremeyev, V. A., "On Natural Strain Measures of the Non-Linear Micropolar Continuum," *International Journal of Solids and Structures*, Vol. 46, 2009, pp. 774–787.

[14]Hodges, D., *Nonlinear Composite Beam Theory*, AIAA, Washington, D.C., 2006.

[15]Yu, W., Hodges, D. H., and Volovoi, V. V., "Asymptotic Generalization of Reissner-Mindlin Theory: Accurate Three-dimensional Recovery for Composite Shells," *Computer Methods in Applied Mechanics and Engineering*, Vol. 191, No. 44, Oct. 2002, pp. 5087 – 5109.

[16]Pietraszkiewicz, W. and Eremeyev, V. A., "On Vectorially Parameterized Natural Strain Measures of the Non-Linear Cosserat Continuum," *International Journal of Solids and Structures*, Vol. 46, 2009, pp. 2477–2480.

[17]Berdichevsky, V., *Variational Principles of Continuum Mechanics*, Vol. 1 and 2, Springer Berlin, 2009.

[18]Lee, C.-Y. and Yu, W., "Variational Asymptotic Modeling of Composite Beams with Spanwise Heterogeneity," *Computers & Structures*, Vol. 89, 2011, pp. 1503–1511.

[19]Dai, G. and Zhang, W., "Size effects of basic cell in static analysis of sandwich beams," *International Journal of Solids and Structures*, Vol. 45, 2008, pp. 2512–2533.

[20]Sharma, A., Sankar, B. V., and Haftka, R. T., "Homogenization of Plates with Microstructure and Application to Corrugated Core Sandwich Panels," *Proceedings of the 51st AIAA/ASME/ASCE /AHS/ASC Structures, Structural Dynamics, and Materials Conference*, AIAA, Orlando, Florida, Apr. 12–15 2010.

[21]Lee, C.-Y. and Yu, W., "Homogenization and Dimensional Reduction of Composite Plates with In-Plane Heterogeneity," *International Journal of Solids and Structures*, Vol. 48, No. 10, 2011, pp. 1474–1484.

American Institute of Aeronautics and Astronautics